Vebjørn Christensen

Numerical calculation of ship appendage resistance using CFD

Master's thesis in Ship Design
Supervisor: Karl Henning Halse
June 2019

Master's thesis

NTNU
Norwegian University of
Science and Technology

Vebjørn Christensen

Numerical calculation of ship appendage resistance using CFD

NTNU
Norwegian University of
Science and Technology

Models now in tanks we tow.

All of that to Froude we owe.

Will computers, fast and new,

Make us alter Euler's view?

Marshall Tulin

Abstract

The object of the thesis is to investigate the added resistance from a bow tunnel thruster, with the help of Computational Fluid Dynamics software. And to find a possible way to estimate the added resistance. The research questions are as follows: What is the added resistance from appendices found in model trials and from numerical simulation? Is it possible to establish a simple, practical, and reliable relation between appendix size and the added resistance on a ship? If so, how well can this practical approach predict the added resistance seen in model tests? To be able to answer those question, Vard Design in Ålesund has shared two of their designs with towing tank results. The design and results are confidential and will not be shown in the thesis.

A Computational Fluid Dynamics program called ShipFlow was used to calculate the resistance. One design was simulated with six different speeds, with six different thruster geometries for each speed. The results were used to calculate a new coefficient for Holtrop's empirical formula for calculating the added resistance of a tunnel thruster. By using Holtrop's equation with the new coefficient, it estimated the resistance of the tunnel thruster for the second Vard model better than the Holtrop equation with the old coefficient.

The equation from Holtrop used was: $R_{BT} = \pi \rho V_S^2 d_T C_{BTO}$, and the coefficient found was: 0,00174592.

Sammendrag

Formålet med avhandlingen er å undersøke tileggs motstanden fra en baug tunnelpropell, ved hjelp av Computational Fluid Dynamics programvare. Og for å finne en mulig måte å estimere den ekstra motstanden på. Forskningsspørsmålene er som følger: Hva er den ekstra motstanden fra vedleggene som blir funnet i modellforsøk og fra numerisk simulering? Er det mulig å etablere en enkelt, praktisk og pålitelig forhold mellom størrelsen og den ekstra motstanden til et skip? Hvis ja, hvor godt kan denne praktiske tilnærmingen estimere den ekstra motstanden som måles i modelltester? For å kunne svare på dette spørsmålet, har Vard Design i Ålesund delt to av deres design med slepetest resultater. Design og resultater er konfidensielle og vil ikke bli vist i avhandlingen.

Et CFD-program kalt ShipFlow ble brukt til å beregne motstanden. Der et design ble simulert med seks forskjellige hastigheter, med seks forskjellige tunnelpropell geometrier for hver hastighet. Disse resultatene ble brukt til å beregne en ny koeffisient for Holtrops empiriske formel for å beregne den ekstra motstanden fra en tunnelpropell. Ved å bruke Holtrops likning med den nye koeffisienten anslås det at motstanden til tunnelpropellen for den andre Vard-modellen er bedre, enn ved bruk av Holtrop-likningen med den gamle koeffisienten.
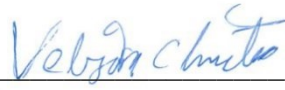
Likningen som ble brukt fra Holtrop er: $R_{BT} = \pi \rho V_S^2 d_T C_{BTO}$, og koeffisienten funnet var: 0,00174592.

Preface

This thesis is the final delivery of a master's degree in ship design at he the Norwegian University of Science and Technology, Department of Ocean Operations and Civil Engineering in Ålesund. With its approval comes the title Master of Science in Ship Design.

The main topic of this thesis is to look at the added resistance from a bow tunnel thruster and to find an estimate for it. The thesis is written in cooperation with Vard Design AS, and the problem was brought up by Kåre Nerland.

Vebjørn Christensen

Stud. Tech – Ship Design

x

Acknowledgements

I would like to use this opportunity to thank the people that have helped me with this master thesis. Firstly I would like to thank my supervisor Karl Henning Halse for helping me with the structure of the thesis and the guidance he has provided. I would like to thank Vard Design in Ålesund and Kåre Nerland for making this thesis possible, by providing me with a problem and material to solve it, and who has been a great help when I have struggled with my CFD troubles. I want to thank professor Henry Peter Piehl for advice for my CFD problems. And also all the professors who have taught me all that I now know, and who have answered all my stupid questions.

I want to thank the support team at Flowtech for fast response to my bugs and errors in ShipFlow, with an extra thanks to Michal Orych, who has responded to most of my emails. I would also thank my classmates who have cheered me on during my five years at the university. I would not have been able to be where I am today without the support of my family and friends and therefore give them a heartfelt thanks. Lastly, I would like to thank my girlfriend for her support during this stressful period.

MASTER THESIS 2019
FOR
VEBJØRN CHRISTENSEN

Numerical calculation of ship appendage resistance using CFD

There are different ways of calculating the resistance of a ship today in the design process. Some are very time consuming and accurate, while others are faster and less accurate. When it comes to estimating the added resistance of appendages, ship companies today use an experience based percentage of the ship hull resistance.

While the percentage resistance added to the total resistance is fast, it is not very accurate. This is especially true for new types of ships, or ships that are different from earlier designs. That is why the industry wants a more accurate but still fast method to calculate the added resistance of appendages. To better calculate the total resistance of a ship.

The scope of this thesis is numerical calculation through CFD software, for the resistance on ship appendages. Limited to bow tunnel thruster and retracted stabilizing fins. The ship type is limited to the ship models provided by Vard.

The objective of the thesis is to present a practical approach that can aid in the calculation of resistance from ship appendices. A practical approach by using CFD will be tested. Afterwards this approach will be used to try to find a correlation between the parameters of the appendage and the resistance.

- What is the added resistance from appendices found in model trials and from numerical simulation?

- Is it possible to establish a simple, practical, and reliable relation between appendix size, shape and position and the added resistance on a ship?

- If so, how well can this practical approach predict the added resistance seen in model tests?

The work scope may prove to be different than initially anticipated. Subject to approval from the supervisor, topics may be added or deleted from the list above or reduce in extent.

The thesis shall be written as a research report, following the template given in Inspera. During preparation of the text, the candidate should make efforts to create a well-arranged and well-written report. To ease the evaluation of the thesis, it is important to cross-reference text, tables and figures. For evaluation of the work a thorough discussion of results is needed. Discussion of research method, validation and generalization of results is also appreciated.

The thesis shall be submitted in electronic version according to standard procedures (.PDF or .ZIP files). Instructions are found on the NTNU website (Inspera) and on Blackboard. In addition to the specified tasks, an A3 poster should be prepared and delivered together with this proposal, and a conference paper will be handled at the end of the research.

After finalizing and delivering the thesis, it must be sent a copy to the supervisor(s).

Deliveries: Final Thesis (11th June)

_____   _____

Vebjørn Christensen   Karl Henning Halse
Student, Ship Design   Supervisor, Ship Design

Table of Contents

List of Figures

List of Tables

Nomenclature

Abbreviations

3D	Three dimensional
BSL	Base line model
CAD	Computer Aided Design
CFD	Computational Fluid Dynamics
EASM	Explicit Algebraic Stress Model
KCS	KRISO container ship
LCB	Centre of buoyancy
RANS	Reynolds averaged Navier-Stokes
SST	Shear-stress Transport model
VOF	Volume of fluid

Symbols

ρ	Density of water
ρ_i	Density of water in imperial units
π	Pi
∇	Differential operator
∂	Partial derivative
A	Area
A_i	Area in imperial units
B	Breadth
C_b	Block coefficient
C_{BTO}	Bow thruster coefficient
C_F	Frictional coefficient
C_T	Total resistance coefficient
C_{TM}	Total resistance coefficient of model
d_T	Diameter of the bow thruster
F_n	Froud number
K_1	Hull form factor
K_2	Appendage form factor
L_{PP}	Length between perpendiculars
M	Million
R_A	Hull roughness resistance
R_{APP}	Appendage resistance
R_B	Bulbous bow pressure resistance
R_{BT}	Bow thruster resistance

R_F	Frictional resistance
R_T	Total resistance
R_{TM}	Total resistance of a model
R_{TR}	Immersed transom resistance
R_W	Wave-making resistance
S_{APP}	Wetted area of the appendages
S_M	Wetted area of a model
T	Draught
V	Speed
$Y+$	Dimensionless wall distance

1 Introduction

1.1 Background

Most markets today are very competitive, and this also applies to the ship design market. There are a lot of different ship design companies, which compete to get design contracts. This drives the designer to produce as fast and as cheap as possible, and still deliver a design within the rules and owner's criteria. A design delivered quickly and with a relatively low cost, are not enough to be fully competitive. The design itself will need to be efficient and cheap to produce. An efficient production can make it easier to deliver the ship on time. The operation aspect of the ship also needs to be considered when a ship is designed. For a ship design to be chosen among the competitors, it needs to be efficient in many areas. The main points are focused on fuel economy and load capabilities. The parameters mentioned above, together with the multitude of companies makes the industry very competitive.

The ship hull resistance plays a significant role in the design of a ship. It mainly affects the choice of main machinery system dimensions. Since with a higher resistance, greater power is often needed to fulfil the operation criteria stated from the owner. The fuel consumptions will also increase with a higher resistance, which in turn increase the demand for fuel capacity. Without increasing the fuel capacity, the endurance criteria might not be met. With increased tank volumes, the loading capacity will decrease, or the ships main dimension would need to be increased. Which in turn, might lead to higher resistance. Those are all points if the ship hull resistance is increased in the design face. However, if the resistance is higher than anticipated when the ship is built, the ship will not perform according to the contract. This could tarnish the reputation of the design company, and they could be fined for not deliver what was stated in the contract. This is why the correct resistance value of a ship hull is essential.

The resistance calculations can be done quickly with empirical formulas. The accuracy of those formulas can vary widely depending on which type of ship they are optimized for. On the other side heavy numerical analysis as Computational Fluid Dynamic analysis, can take a significant amount of time and computational resources. The skills of the person doing the set up for the Computational fluid dynamics has great importance because the simulation is sensitive to how the mesh is modelled and what kind of solvers are used. However, when the CFD simulation is set up correctly and the computation power and time are available, the results tend to be accurate.

It is the factors mentioned above that is the background and motivations for this thesis. The industry needs a fast method to estimate the added resistance of the appendages. One of the uncertain components is appendage resistance. Today an estimate based of the percentage of the total resistance is used. The percentage used are from earlier experiences. This is limiting when new ships that are not similar to earlier designs will be developed. That is why a different method for estimating the added resistance is sought after.

1.2   Objective and research questions

Research question

   - What is the added resistance from appendices found in model trials and from
   numerical simulation?
   - Is it possible to establish a simple, practical and reliable relation between appendix
   size and the added resistance on a ship?
   - If so, how well can this practical approach predict the added resistance seen in
   model tests?

1.3   Scope
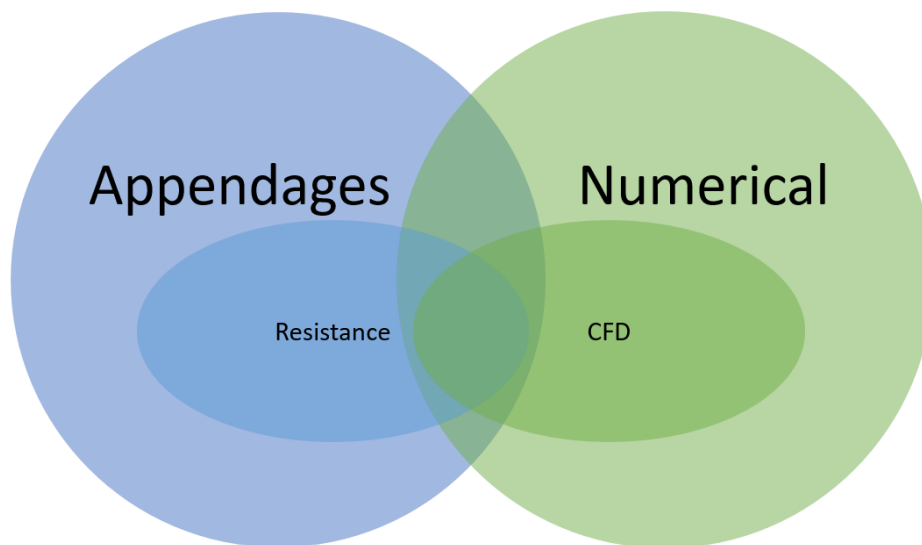
Figure 1-1. Venn diagram of the scope.

The scope of this thesis is shown in Figure 1-1. It will focus on the main topics numerical
calculation, and appendages. However, those are limited to looking into the resistance by
doing CFD simulation and looking for a correlation between resistance and a few
appendage parameters.

The appendages are restricted to ship appendages. There are a lot of different
appendages on different type of ships. The scope of the appendages is restricted to only
include bow tunnel thruster with a grid. The appendage parameter that will be looked
into are the diameter of the tunnel thruster.

1.4   Structure of the thesis

The thesis is divided into different chapters. Chapter one is the introduction. The second
chapter will go into the theory used, with subchapters detailing the essential parts. For
the third chapter, the method is presented, to give a clear explanation of how the
problem will be solved. The fourth chapter contains the study cases. While the fifth
chapter includes the results and discussion parts. The last chapter will talk about the
concluding remarks and further possible work.

2 Theory

2.1 Bow tunnel thruster

There are many different types of appendages on modern ships. They all have their function and form. The shape of those components adds geometric complexity to a standard hull. The new geometry will influence the resistance of the ship with different degrees depending on the shape. Because this thesis only looks into the resistance from bow thrusters, it will be the only appendices discussed in this chapter.

Manoeuvring can be a problem for some large ships. Like for cruise vessels, that needs to manoeuvre in relatively tight places and harbours. The rudder placed behind the propeller for usual manoeuvring is often not enough when sailing in narrow places, or when docking. One way of solving this is by adding thrusters in the bow section of the ship.

Tunnel thruster puts a propeller inside a tunnel in the bow region, which is placed normal to the ships centre line. So that it can provide side way thrust. The thruster unit is often located in the middle of the tunnel, and the opening often has grating as shown in Figure 2-1. To protect the unit from objects in the water that could damage it. (J. Carlton, 2012) also says, the grating also serves the purpose to dampen the hydrodynamic forces on the back wall of the tunnel, and therefore also reduce the resistance. The bars create turbulent flow instead of laminar flow, which is advantageous with regards to the resistance mentioned earlier. The bars in front of the tunnel openings are a mix of horizontal bars and vertical flat bars. The thrusters are placed beneath the water line, generally as far down as is feasible to reduce the risk of the propeller sucking air.

Figure 2-1. Picture of three bow tunnel thruster. (Hochhaus, 2012)

Different types of bow thrusters can be used for manoeuvring. Another type is the retractable azimuth thruster shown in Figure 2-2. When the ship is in regular transit, the thruster is retracted into the hull for low resistance, relative to what would have been if it had stayed out. Another similar thruster is one that swings up into the hull. An advantage for a retractable thruster that can rotate 360 degrees when deployed is that it can be used as a propulsion unit. This enables it to sail the ship to a safe place in an emergency if the main propulsion units fail.
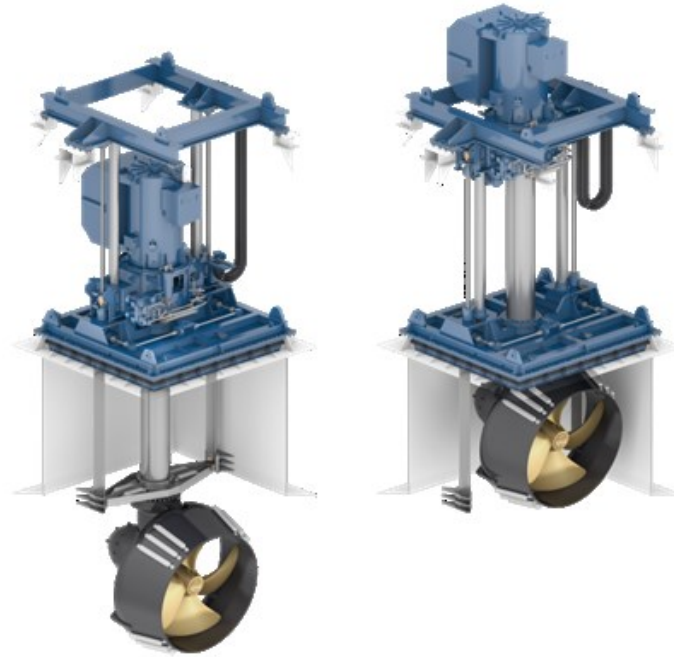
Figure 2-2. Retractable thruster. (Wärtsilä, 2019)

(House, 2007) mentions a different solution, which is to combine the retractable azimuth thruster with a tunnel thruster. That kind of thruster is called a combi thruster. They usually are retracted into the hull, where the thrust direction is normal to the centreline of the ship, and a tunnel is cut out of the hull to allow the thruster to operate as a regular tunnel thruster. If a situation demands more precise manoeuvring the unit can be lowered down to provide better manoeuvring. In the outer position, it will be able to provide thrust in 360 degrees. With this kind of thruster, there will be three holes in the ship. Two holes for the tunnel, and one underneath for where the unit is lowered down or hoisted up. This would create more areas that could increase the resistance of the ship.

2.2 Ship resistance

There are many aspects to consider when designing a ship. One of the aspects is the resistance of the ship. Other aspects are structure calculation with regards to strength and weight. The stability analyses of a vessel are of great importance because a failure in the stability calculation can lead to loss of human life in the worst case. Weight of a vessel is determined by the volume of steel used and how large the machinery systems are, together with the cargo load. The weight is an essential aspect of ship design because it is linked with build cost, loading capacity, and performance. As well as other aspects.

All those aspects above are linked to the resistance of the ship. The strength calculation has a direct connection with the length of a ship, and the same goes for the resistance. Because the resistance is linked with the Froud-number, which are linked with the length of the ship. To get low resistance a long ship relative to its size is wanted, but this might increase the requirement for longitudinal strength, which would increase the weight. The same goes for the stability. In general ship design practice, a narrow ship usually has a lower resistance than a similar sized ship with a higher B/T ratio. To fulfil stability requirements, the breadth needs to be large enough for the given ship. This is just some of the connections that shows that a correct resistance estimate, is necessary for the ship design process.

To better understand the resistance, it is needed to know where the resistance comes from. The total resistance of a ship is made up of different parts and divided into two main groups, as shown in Figure 2-3.
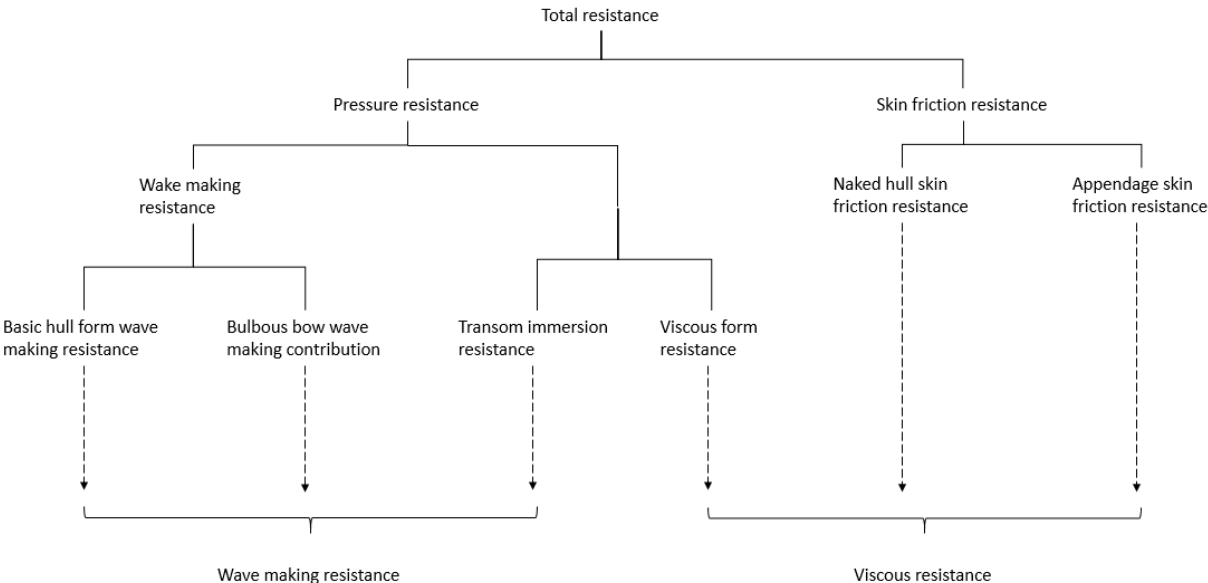
Figure 2-3. Resistance components of a ship. (J. S. Carlton, 2007)

The resistance can be split into two parts as seen in Figure 2-3. The skin frictional resistance is components of tangential shear forces that work on the hull. Pressure resistance comes from the pressure force working on the hull. The pressure and shear forces are different in a different part of the hull. The reason for this is the shape of the ship and the incoming flow around the vessel. The two components can be divided into even more parts for a more detailed understanding. From this detailed breakdown, it is possible to simplify the components back to two main resistance components. The reason why this is done is that if the wave forces are known, the wave pattern can be investigated. The design can then be changed with regards to the wave pattern, to minimize the forces from the waves. Appendages close to the surface, might change the pressure around the ship body, and might therefore increase the resistance of the ship.

The resistance components shown in Figure 2-3 are a simplified version, a more comprehensive representation are shown in Figure 2-4. All the components mentioned are not necessary for this thesis, therefore are the more straightforward representation used.
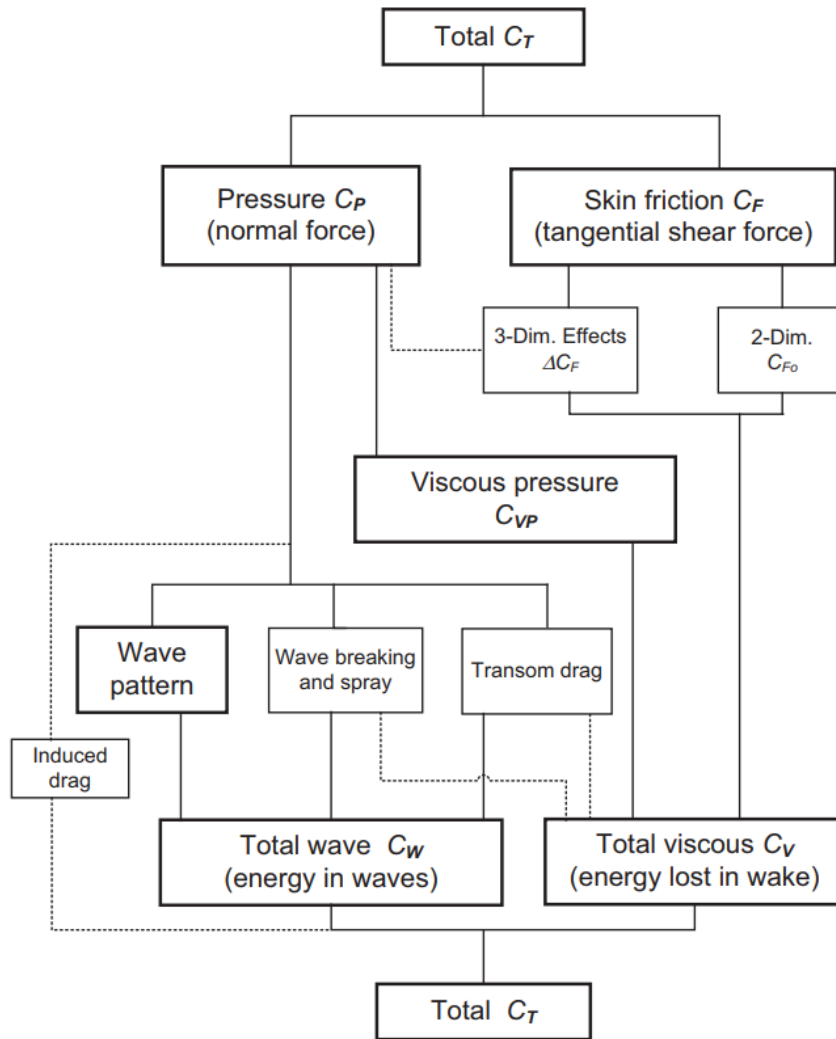
Figure 2-4 Complex total resistance components of a ship. (Anthony F. Molland, Stephen R. Turnock, & Dominic A. Hudson, 2011)

For calculating the total hull resistance (J. S. Carlton, 2007) has listed Holtrop's empirical formula based on 334 model test. The complete formula is shown in equation 2-1. The added resistance is given by one part and is comprised of several parameters as is shown in equation 2-2. A formula for the added resistance of the tunnel thruster can be found in the appendage formula and it is shown in equation 2-3. Where the coefficient C_{BTO} is a coefficient based on results from the model test.

$$R_t = R_F(1 + K_1) + R_{APP} + R_W + R_B + R_{TR} + R_A \qquad \textbf{2-1}$$

$$R_{APP} = \frac{1}{2}\rho V_S^2 C_F(1 + k_2)_{equv} \sum S_{APP} + R_{BT} \qquad \textbf{2-2}$$

$$R_{BT} = \pi \rho V_S^2 d_T C_{BTO} \qquad \textbf{2-3}$$

A different and much simpler formula for estimating the resistance of the thruster, was proposed by (George R. Stuntz, 1964) and are shown in 2-4. However, since it is from the USA and are so old, the formula is meant for imperial- and not metric values as are used in the rest of the thesis.

$$R_{tunnel} = \frac{0.07\rho_i}{2} A_i V_{knots}^2 \qquad \textbf{2-4}$$

After finding a resistance either for the whole ship or for just the appendage, it can be useful to change it from Newton to a dimensionless coefficient like C_T, which are the coefficient for the total resistance. Equation 2-5 from (ITTC, 2002) helps convert the total resistance of a model ship from Newton to the dimensionless resistance coefficient C_{TM}.

$$C_{TM} = \frac{R_{TM}}{\frac{1}{2}\rho_M S_M V_M{}^2} \qquad \textbf{2-5}$$

2.3   Numerical

In this chapter, the fundamentals of numerical calculation of resistance will be presented, together with essential components that are necessary to do the calculations.

2.3.1 CFD

"Linear approaches, such as standard strip theory methods and panel methods, are appropriate to solve many ship seakeeping problems, and they are frequently applied. These procedures are fast, and thus they allow investigating the effect of many parameters (frequency, wave direction, ship speed, metacentric height, etc.) on ship response. Nonlinear computations, such as simulation procedures based on Reynolds-averaged Navier-Stokes equation (RANSE) solvers, are necessary for the treatment of extreme conditions." (El Moctar, 2008)

As stated in the quote above, the linear approaches are favourable for more standardized problems. Because they are fast, and the results are good enough to be used. However, when the problems get more complicated, or the industry demands higher accuracy Computer fluid dynamics or CFD for short are a preferable option. The computational and time demanding Reynolds-average Navier-Stokes equations are one of the most used solvers for CFD programs.

The CFD is known to be able to give accurate results. However, that is not given, because of the high complexity in doing a CFD simulation. The number of steps and decisions that needs to be right are by far more than the number in more traditional linear methods. (A. F. Molland, S. R. Turnock, & D. A. Hudson, 2011) The uncertainty of the results is also an important part to notice. Because the model is limited by the inputs and the mathematical models and, therefore, not able to represent the correct physical laws as in the real world. For a correct setup, that can simulate the laws of physics close to the real world, the potential for accuracy is good.

Three general conservation laws govern the flow around a ship. The laws are the conservation of mass, momentum, and energy. Together they form the Navier-Stokes equations. This is the governing equation for a fluid. (Bhaskaran & Collins, 2002) From (A. F. Molland et al., 2011) the first equation (2-6) states that in an infinitesimally small control volume, the rate of change of mass is equal to the rate of mass flux through the boundary surface. The second equations (2-7) states that the rate at which momentum is entering or leaving through the surface is equal with the rate of change in momentum in the control volume, with the additional sum of the forces acting on the volume itself. The last part of the Navier-Stokes equations is the energy equation (2-8), which states that the viscous stress and work done on the control volume together with the rate enthalpy is entering, are equal to the rate of change in internal energy in the control volume.

$$\frac{\partial \rho}{\partial t} + \nabla \cdot (\rho V) = 0 \tag{2-6}$$

$$\frac{\partial(\rho u)}{\partial t} + \nabla \cdot (\rho u V) = -\frac{\partial p}{\partial x} + \frac{\partial \tau_{xx}}{\partial x} + \frac{\partial \tau_{yx}}{\partial y} + \frac{\partial \tau_{zx}}{\partial z} + \rho f_x$$

$$\frac{\partial(\rho v)}{\partial t} + \nabla \cdot (\rho v V) = -\frac{\partial p}{\partial y} + \frac{\partial \tau_{xy}}{\partial x} + \frac{\partial \tau_{yy}}{\partial y} + \frac{\partial \tau_{zy}}{\partial z} + \rho f_y \tag{2-7}$$

$$\frac{\partial(\rho w)}{\partial t} + \nabla \cdot (\rho w V) = -\frac{\partial p}{\partial z} + \frac{\partial \tau_{xz}}{\partial x} + \frac{\partial \tau_{yz}}{\partial y} + \frac{\partial \tau_{zz}}{\partial z} + \rho f_z$$

$$\frac{\partial}{\partial t}\left[\rho\left(e + \frac{V^2}{2}\right)\right] + \nabla \cdot \left[\rho\left(e + \frac{V^2}{2}\right)V\right] = \rho \dot{q} + \frac{\partial}{\partial x}\left(k\frac{\partial T}{\partial x}\right)$$

$$+ \frac{\partial}{\partial y}\left(k\frac{\partial T}{\partial y}\right) + \frac{\partial}{\partial z}\left(k\frac{\partial T}{\partial z}\right) - \frac{\partial(up)}{\partial x} - \frac{\partial(vp)}{\partial y} - \frac{\partial(wp)}{\partial z} + \frac{\partial(u\tau_{xx})}{\partial x}$$

$$+ \frac{\partial(u\tau_{yx})}{\partial y} + \frac{\partial(u\tau_{zx})}{\partial z} + \frac{\partial(v\tau_{xy})}{\partial x} + \frac{\partial(v\tau_{yy})}{\partial y} + \frac{\partial(v\tau_{zy})}{\partial z} + \frac{\partial(w\tau_{xz})}{\partial x} \tag{2-8}$$

$$+ \frac{\partial(w\tau_{yz})}{\partial y} + \frac{\partial(w\tau_{zz})}{\partial z} + \rho f \cdot V$$

In equation 2-6 the ∇ is the differential operator $(\frac{\partial}{\partial x}, \frac{\partial}{\partial y}, \frac{\partial}{\partial y})$, and $V = (u, v, w)$ in equations 2-7. For equation 2-8 the $V^2 = V \cdot V$.

There are only a few analytical cases that can be solved by the Navier-stokes equations, for other cases a numerical solution needs to be used. To be able to use it for practical problems, some assumptions need to be made. With assumptions, the computation needed can be reduced, and therefore make it more feasible. One of the methods to simplify the Navier-Stokes equations are the RANS method.

The RANS method is well used, as mentioned earlier, but it is still a complicated method. It is based on the Navier-Stokes and uses some assumptions to be able to be applicable in real-world related problems. Molland mentions the assumption that is made is that the flow in the control volume is incompressible. With this assumption, it is possible to simplify the continuity- and momentum equation, while the energy equation can be disregarded entirely. The three velocity components are assumed then to be simplified into rapidly fluctuating turbulent velocities that are around a slowly varying mean velocity. This assumption gives six new terms, which are known as Reynolds stresses. To get the stresses to work with the mean flow, a turbulence model is introduced to represent the interaction.

2.3.2 Turbulence model

The turbulence also needs to be considered. This is done by implementing a turbulence model, which represents the interaction between an underlying flow and the Reynolds stresses. Turbulence is a complex phenomenon and is not fully understood. The turbulence models are therefore semi-empirical, which gives room for errors. The necessity for a perfect representation of the turbulence flow in the whole flow domain is maybe not necessary for engineering purposes according to (Bertram, 2012).

There are many turbulence models, but the most used by commercial applications are the $k - \varepsilon$- and $k - \omega$ model. (Menter, 1994) said at the time it was four main groups of models. The first are the algebraic models, then comes the one-equation models, followed by two-equation models, with second-order closure method as the last one. The models mentioned first in this section belongs to the two-equation models. Since they are some of the fundamental models in the two-equation models, others have emerged. Such as the Base line model or BSL, and Shear-Stress Transport model or SST.

2.3.3 Boundary condition

When looking at the resistance in a ship the ship is often looked at within a large body of water, so that the flows around the hull can develop correctly and that it will not be affected by external factors. In an ideal simulation, this should have been done, but then the computational domain will be too large to handle. The boundary condition is therefore applied to the outer borders of the domain so that they mimic the real world. This is done by applying a specific condition on the side- and bottom boundary. A specific condition could be to use a symmetry plane. By using symmetry all the derivatives in the normal direction and the normal velocity are set to zero. The shear stresses are then set to zero. Specific values computed for the outer layer could also be used. This could also reduce the total domain, but since the cell size are so large in the outer areas, the total number of cells would not decrease with any significance.

The ship hull also needs to define the boundary condition. By using the no-slip condition on the hull side, which means zero relative speed as stated by (Bertram, 2012). The hull will get the correct conditions. Depending on the turbulence model used, the no-slip condition is applied by enforcing it directly or via a wall function. For the inlet and outlet walls, they need a different condition. The wall in front of the ship needs to simulate the inflow that the ship goes through. This is done by specifying all the unknowns at the inlet. For the outlet, it needs to keep the flow leaving the domain so that the continuity is preserved for the whole fluid domain.

3 Method

This chapter contains the general method used to find the needed results, as well as the method for the CFD cases. It will also consist of some elementary theory on ShipFlow, and it will include the method on how to find an estimated value for the added bow tunnel thruster.

The method used in this thesis that tries to answer the research question is presented shortly. To begin, a relatively simple ship was chosen. The ship had some information available to help in the investigation of the reliability of the results, such as test tank results. Next was to find a setup that could be simulated in the ShipFlow software without needing too much computational power. After a successful simulation, the results would need to be checked with experimental results, and if they were not within a reasonable value, the setup would need to be changed and improved before the simulation was done again. This would be done until a satisfactory resistance result was found.

The next step was to repeat the same procedure on the model dispatched by Vard. If the method used earlier was good enough, the next step was to change the thruster size and compare results. By using equation 2-3 from Holtrop, it was possible to find a coefficient for every case of the different tunnel thruster sizes and speeds, then the average of all the coefficients was found.

3.1 ShipFlow

To be able to calculate the resistance from a bow thruster, a suitable method must be used. The RANS-method has been mentioned earlier and is a useful tool for resistance calculations. However, to solve the RANS-equations more tools are needed. Several programs are created to calculate the flow and resistance for ships. Some of them are Star CCM+, OpenFOAM, FLUENT, and ShipFlow. They all are CFD programs, but still very different. This is important to know when one needs to choose a code to solve a problem. Star CCM+ is a program with a lot of option and possibility, and the user needs to input and make all the choices. On the flip side, ShipFlow requires little input to be able to run a resistance simulation. This might be the reason why ShipFlow is used in the industry. Also, why VARD wanted it used for this thesis.

The software has different internal programs and solver. The main option is to use the Xpan, Xchap, or both programs. When the Xpan keyword is implemented, the simulation will start with a potential theory calculation. Moreover, if the Xchap keyword is used, it will only use the RANS equations. However, when both are used, it will first calculate the potential equation, and then solve the RANS-equations for the chosen domain. The starting values for the RANS-equation will then be based on the results from the potential theory. If the user wants to use the volume of fluid methods, this is possible but needs to be specified.

3.2 Practical process

When doing a CFD simulation, a general method is to set up the case. This method starts by importing the 3D model, then converting the model into a mesh that represents the geometry. After that, the domain for the computations needs to be specified, usually a box or cylinder that covers the whole model. When this is done, a mesh needs to be created inside the domain, where the mesh size needs to be established. Refinement zones then needs to be implemented around the model and in areas that are important for the flow development, such as behind a ship, in the surface, or around intricate geometries. When all this is done, the solver needs to be chosen, and parameters that are important for the case should be stated for the solver. After the simulation has been stopped by either the program itself or the user, the results and data need to be investigated. This is to see if the solution has converged and that the results seem plausible compared to earlier experience or experiments.

Below are the different steps explained further with the program ShipFlow in mind and how ShipFlow does some of the steps. Since ShipFlow is made different than other CFD programs the steps explained earlier are not followed in the same order. Instead, most of the inputs can be done at once if the values are known for the user. The method is therefore explained in the order that is normal to do in ShipFlow.

3.2.1 User interface

The program ShipFlow is a commercial computational fluid dynamics software that aims to help corporations to solve their hydrodynamic calculation for ships. This is evident when looking at the user interface since it is easy and clean. As can be seen in Figure 3-1 where all the decisions and values are inputted in the left side, and the representation of the hull, in this case, is shown in the large window on the right. For the left side, keywords are used for different menus, those keywords are the same that are used in the output file and configuration file. When a keyword is chosen it is implemented, and this can lead to changes in the simulation. A list of the keywords are listed in Table 3-1, with a short description. The words listed to the far left are the main keywords. The second keyword listed in the middle can implement new parameters that the user can change as is shown in Figure 3-2 where all the keywords for the setup are shown, and vship which are highlighted have its option in the upper part. There it is possible to change the values for the Froud number and Reynolds number. More options could be chosen by using the rolldown window in the top of the figure, where vknot is located.

Table 3-1 List of different keywords used. (Flowtech, 2019)

Keywords	Description
xflow	Start keywords, which are always included
title	Title
program	Which modules of ShipFlow to run
vship	Speed of ship
hull	Specify the type of ship and specify input for the standard case option
offset	Name of the file containing hull offsets or iges, orientation and size of the hull in the offset file
fluid	Fluid properties
tunnel	Tunnel properties
xgrid	Generates the grid used for the viscous computations in xchap
size	Number of clusters in the final grid
singul	Location of the singularity lines (parametric edges between the wake surface and the two η-boundaries).
xchap	Starting a finite volume code that solves the Reynolds averaged Navier-Stokes equations
control	Specify execution mode and maximum number of iterations.
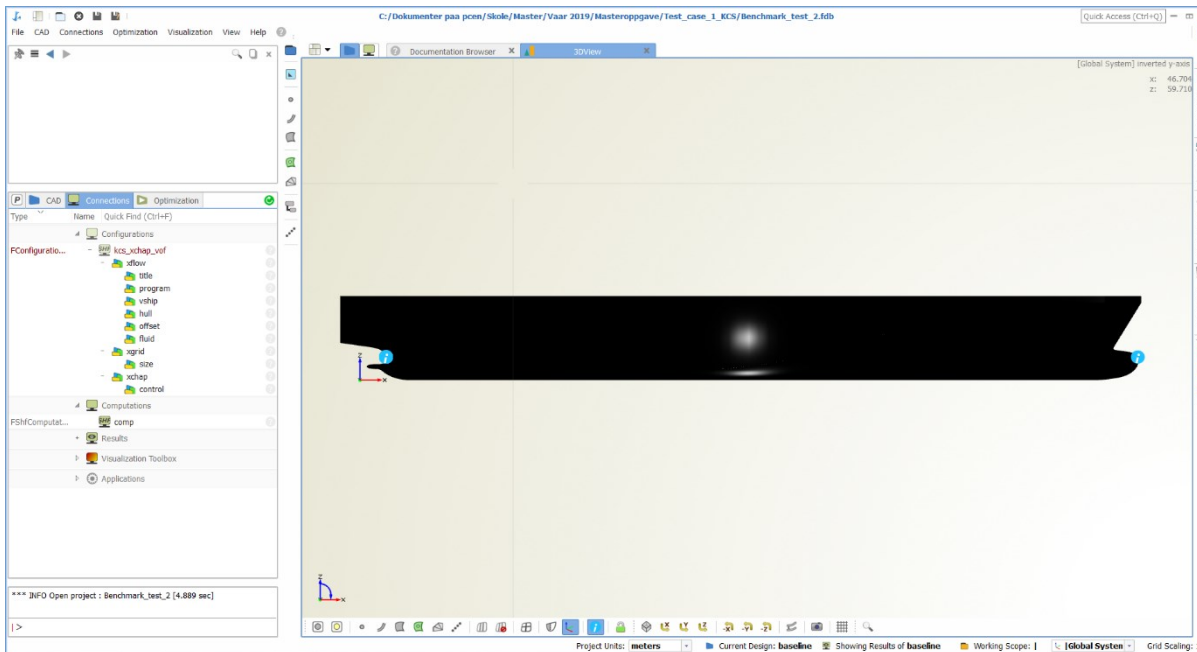
**Figure 3-1 Illustration of the main window in ShipFlow.**
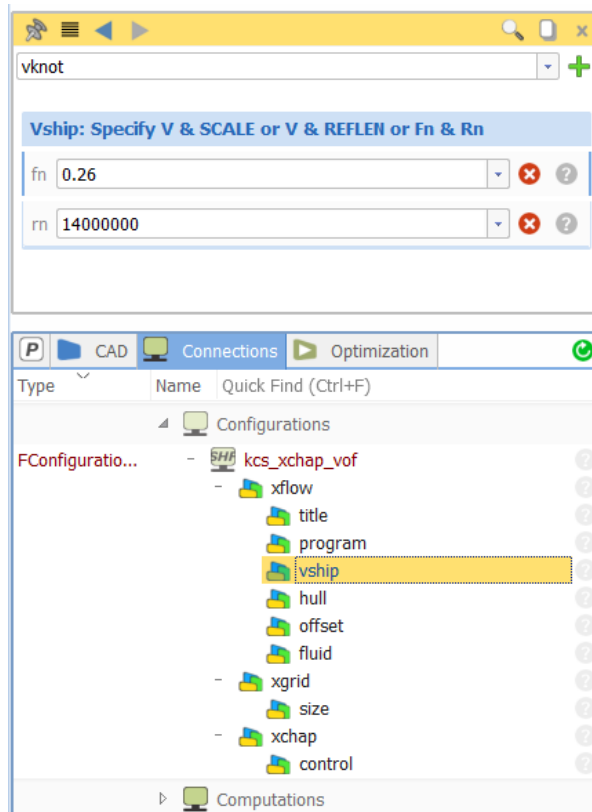
Figure 3-2 Illustration of the menu layout and input.

The right side of Figure 3-1 is used to represent most of the visual results, and the tables that contain the results, and also the full report of the simulation when it is done. For a calculation, the different elements needed for the calculation needs to be implemented. This ensures that only the necessary parts of the software are used, and therefore saves computational power. After choosing the main parts for the calculation some minor decision will need to be done, but the rest will use their default values if its not specified otherwise by specific keywords. The values are chosen by Flowtech the company that creates ShipFlow, and with their several years in the industry, it can be assumed that the default values are a good starting point. However, if any errors or inaccuracies occur, the default values will need to be changed to fix the problems. This is when the program goes from a simple and straightforward software to a more complex CFD program with many possibilities.

Some of the possibilities and choices are the choice between the use of potential theory or RANS-equation calculations. One can also only use RANS in a limited part of the domain to save computational power if only the flow field in the aft ship is what is investigated. If RANS is chosen a lot of new small variables can be selected, such as the turbulence model, the Y+ target, the convergence criteria, if there should be free surface, or use the volume of a fluid method to mention some.

3.2.2 CAD model

ShipFlow does not make ship hull geometry models, so to get a geometry into the program it must be imported from another software. The program supports several different file formats, such as IGES, SAT, STEP, PARASOLID, Offsets, and OpenNURBS. From one of those files, the program can create its own geometry, which they call an offset file. This is probably to make it easier for the software to interpret the geometry. Different file formats can have different qualities, and this is a step to prevent that. Without this step, complex geometry might not be represented in the correct way for the solver. A transition between an external file format and the solver is then needed, and that is where ShipFlows own offset file is used. It uses the existing file and then creates lines in the transverse section along the hull as shown in Figure 3-3. This gives the option for the user where to refine the distance between the lines in the longitudinal direction. So that for part of the hull with considerable complexity a small distance between the lines can be used to capture all the geometric shapes. Alternatively, where the changes in form do not differ, a larger distance can be used to save file size. This is evident in the figure below, where the left side is the aft ship and have a large density of lines relatively from the right side, which are the midship.
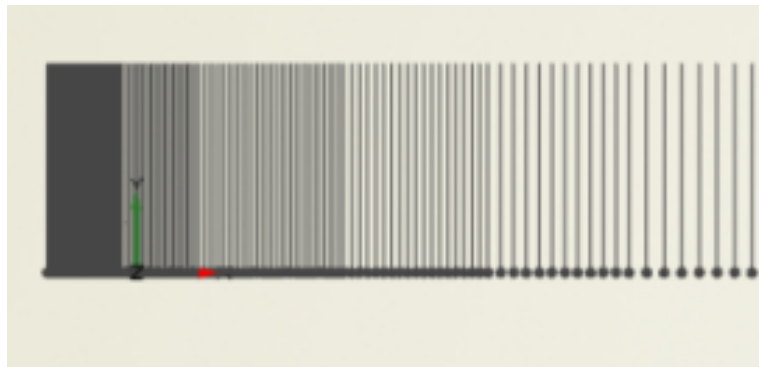

Figure 3-3 Illustration of the output from the offset file. Taken from the aft ship.

It is essential with a good three-dimensional model of the hull to get the correct form. A model with low quality might not have the correct angels or transitions, needed to simulate the flow correctly. Which in turn, will give a false representation of the resistance. This can be hard to spot on the initial models. However, if the model is looked over carefully with a focus to find irregularities, it could be possible to find the larger and more impactful imperfections. To improve it can be more difficult, because the CAD software used might not be good enough, or the experience to solve the problems might not be available. That is why having different option for creating the hull geometry can be beneficial. So that the form can be presented in the most correct way possible as mentioned by (Petersson & Chand, 2001).

The importation of a 3D model into ShipFlow is easy, but the conversion into the offset file can be tricky. Since it requires some unintuitive commands that are not easily explained in the tutorials.

3.2.3 Thruster

If any appendages are to be implemented, it can be done after the importation of the model. In this case, that appendage is limited to the forward thruster. To add a thruster the sub keyword: tunnel needs to be added under the main component Xflow. By adding this part, the software knows that a thruster is implemented. All the dimensions and descriptions of the geometries then need to be specified. A protective grid can, as mentioned before, reducing drag and is, therefore, an important aspect to take into account. Some of the parameters that can be changed for the protective grid are shown in Figure 3-4. The protective bars are also one of the places that errors are likely to occur. This can happen in the form of leaks. Wrong values for this part will give a wrong geometry of the thruster, which could give the wrong flow field.
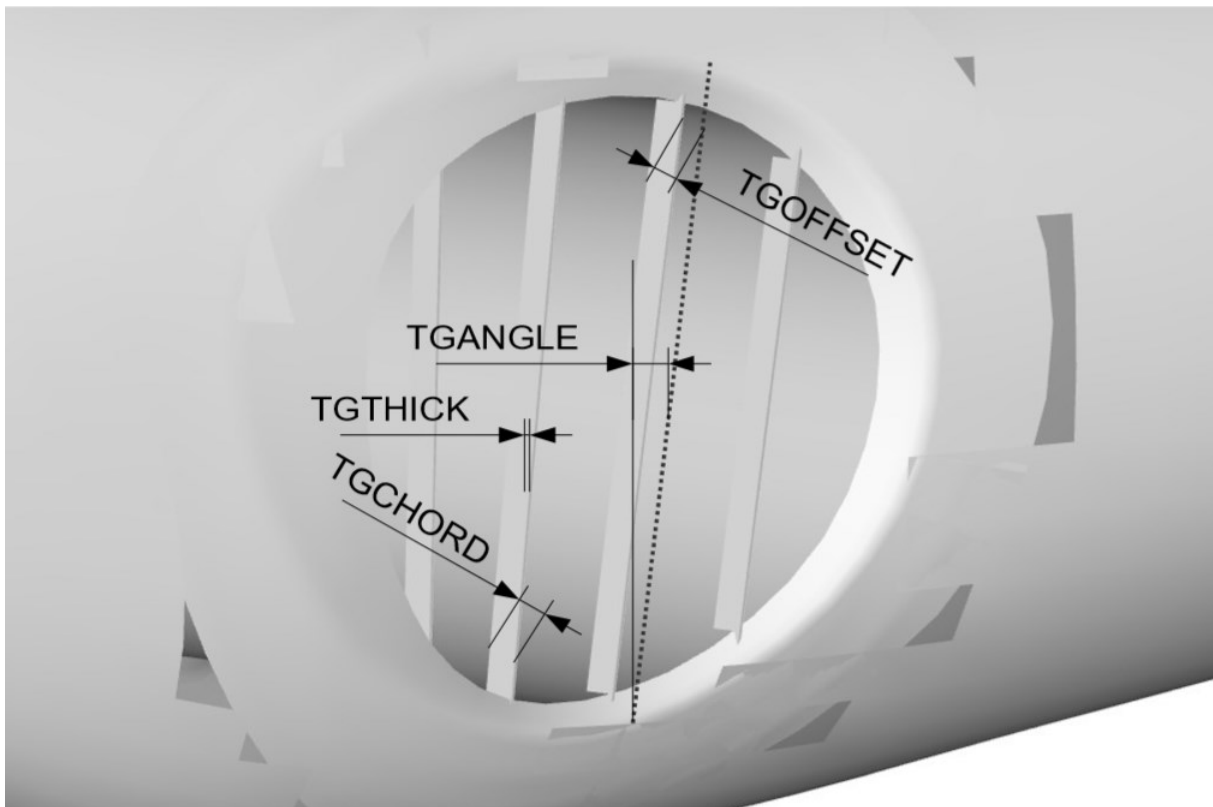
Figure 3-4 Geometric parameters for the protective grid (Flowtech, 2019)

The way the thruster implementation works is that it takes the thruster dimensions specified and creates a mesh. It is this grid that represents the characteristics of the tunnel. This means that changes to the thruster can be easily implemented without having to change the main CAD file for the hull. The problem with this method is that a mesh is not perfect, and this is where the errors and wrong flow fields as mentioned above could occur. However, a mesh would have needed to be created even though the thruster had been made in the original 3D model. The difference is that it is now possible to change the values for both the thruster and mesh size in one place.

3.2.4 Meshing

After importing a geometry into the program, a mesh needs to be applied. This mesh will be the starting point for the numerical calculations done by the software. There are different ways to apply a mesh to a structure. One way is to let the user create many zones and decide the mesh size individually in each of them. This gives the user great control over the meshing operation and is called structured mesh. However, that will also leave the possibility of user error, or small mistakes that can contaminate the setup. The other way of creating a mesh is to let the computer create it with only controlling the cell-size and refinement zones.

The method used will vary significantly for different programs. The procedure used by ShipFlow is somewhat of a hybrid. ShipFlow will create a grid if nothing about the mesh is stated, but by adding the keyword Xgrid, it is possible to add several new keywords with sections where it is possible to include specific commands or change some parameters.

The program uses a Poisson solver to create the mesh for the CAD model. Then if the keyword: global are used, it creates a large cylindrical mesh around the model. When implementing the mesh, the user can use the predefined sizes ranging from coarse, medium, and fine. Those keywords have predefined values for the distance from the forward part of the model and to the frontal wall. The same goes for the length from the back of the model and to the back wall. This is shown in Figure 3-5, where the upper letters represent the zones, and the names at the underside represent the start and end of the zones. The letter at the top side decide how many planes there should be in their respective area in the axial direction, and the letters at the bottom are stated by using the distance from the forward perpendicular of the ship, with values that are stated in the model's length, were the positive direction is from bow to stern. The standard value for xstart is – 0.8. Even though they have predefined values from the initial keyword. The user can change each individually to meet the needs of the problem. For a standard ship resistance calculation, the distance from XSTART up to forward perpendicular is recommended to be around the same distance as the length of the ship. For the back part, XEND is recommended to be located two times the ship length behind the aft perpendicular. This is done not to get any backflow, and to get a better developed wake.
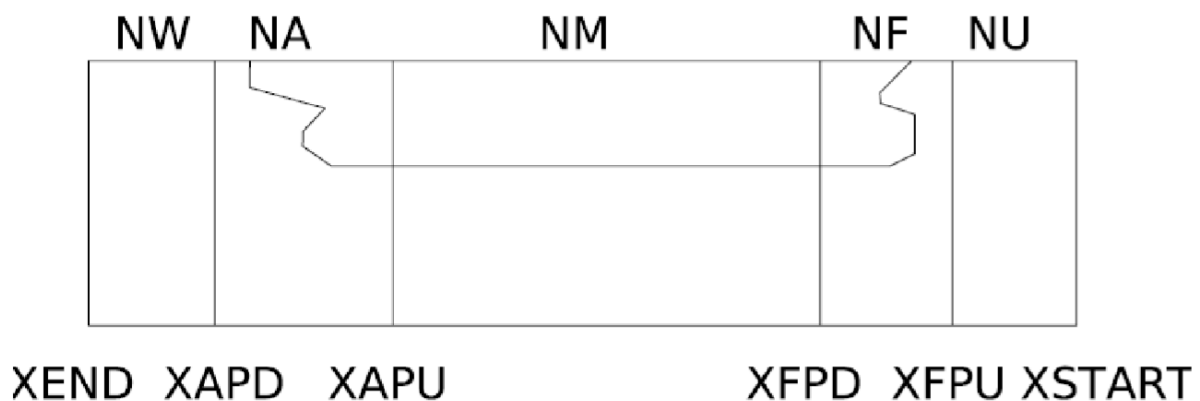
Figure 3-5 Meshing zones in the longitudinal direction (Flowtech, 2019)

The radial dimension of the domain can be controlled by changing the radius. This distance is advised to be around the length of the model. Those are just the main dimensions of the domain, and some of the possibilities. An illustration of a possible domain is shown in Figure 3-6. To further refine the mesh, the number of planes in a different direction can be defined. By choosing either, coarse, medium, or fine mesh the number of planes in radial and circumferential direction are preselected. The number of planes in the axial direction in the areas shown in Figure 3-5 are also defined in the keywords mentioned. Those are the preselected parameters that need to be changed to refine the mesh in specific places and are the only way to do so without importing a mesh from other software. The method talked about above uses a global mesh, that solves the RANS-equation in the whole domain, but it is also possible to limit this to only some part of the domain. That requires that the rest of the domain is solved by another method than solving the RANS-equations.
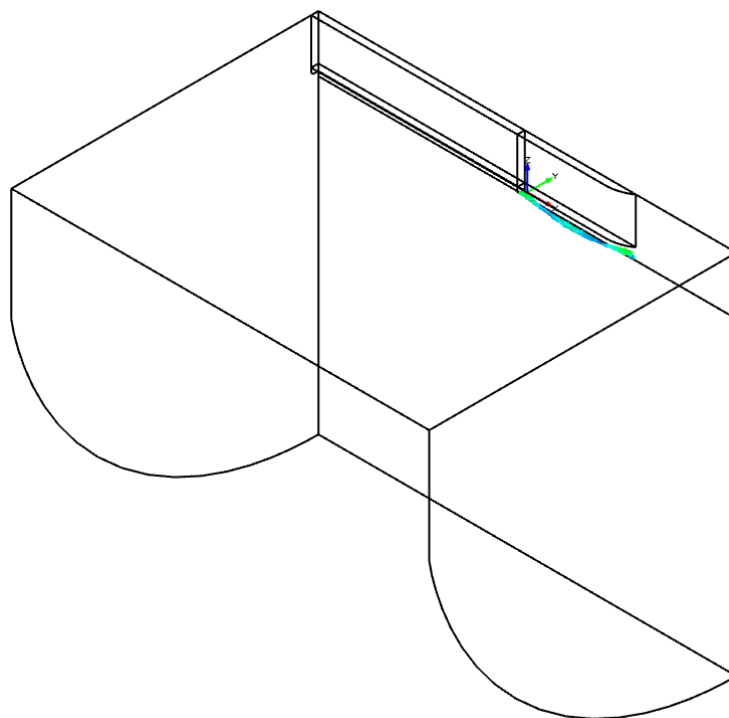
Figure 3-6 Illustration of half of a cylindrical domain, with zones for the upper side- and back side of the ship.

3.2.5 Post processing

When the calculation is done, the post-processing needs to be evaluated. This can be done by looking at the residuals, the flow field, or the results. The residuals are plots that show the change of different values, such as the friction and pressure in x-, y- and z-direction. As well as the momentum in x-, y- and z-direction. If the individual lines go down and below one and also converge, it is generally a valid run for that setup. Generally, in many cases, the user would have to look up the residuals and try to interpret the graphs. The decision if it looks good enough fall upon the user, while in ShipFlow the program as a default value set for the convergence. This solution can be both positive and negative. It makes it easy for the user when the solution converges. However, if the solution does not converge, it gives no help as to what might be the issue. The user must then check the residuals to try to locate where the problem can be.

3.3 Equation creation

Doing a full CFD simulation can be time demanding since the time it takes to set up can be long, and the time for the simulation itself can also take a long time depending on the computational power. Using an equation takes a shorter time, but it might not be as accurate. It depends on the type of equation. A CFD simulation is many equations that are solved numerically. The completely different type is the empirical equations, such as the one mentioned in chapter 2.2. This type of formula can be useful at the beginning of the design process since it can give a quick estimate.

An empirical formula is limited to the amount of data the equation is based on. The more data the more accurate or average the coefficients in the equation would be. And the more changeable values can be included. However, to do this, it requires many values for different designs. The Holtrop formula is based on 334 model tests. A model test takes a lot of resources to be done right, which makes it hard to do a lot of different small changes on a design and do this on many designs. However, this could be done within a CFD program if the results are within acceptable values.

Using a CFD software to test many different thruster designs on a model, where the size, position, angles, and number of bars would be changed would be ideal since this could lead to an equation that takes all of those parameters into account. When looking at the tunnel thruster resistance, the first step would be to start with one suitable model and find its resistance without the tunnel through a CFD program. Then the next step would be to add a tunnel thruster and use the same setup, with the only difference that the thruster is included. And run those two setups at a range of speeds. By subtracting the model without the tunnel from the model with a tunnel, one would get the added thruster resistance. By doing this for all the speeds simulated and then checking how well that matched a towing tank test could validate the method. If the method for the CFD was a general method without any special consideration in the setup, it could be applied on similar designs. And by doing that, one could find a coefficient for an equation that was dependent on speed.

To get a more accurate equation, the same method could be done, but for every speed tested. Different sizes in the thruster design would let the equation be dependent on both speed and size. By continuing this method and applying more parameters, the equation could become more accurate for tunnel thruster estimate. And by using the method on different ship design, the coefficient calculated would be more accurate.

4 Study cases

This chapter will talk about the different cases investigated in this thesis. It will investigate the small details needed to recreate the different cases. The first case is to try a known ship model, with results available by other studies. This is to find the correct method to use in the program that is intended to be used. The other cases are based on a model provided by VARD Design. Here the method used in the earlier case will be used, and then the results will be compared to the model tests done by VARD.

This thesis has been made possible with the help of Vard Design in Ålesund. They have supplied ship models and towing test results for the given models to be used in the simulation. However, since they are a commercially driven company, the material provided by them will not be shown. This is not to reveal any of the details in their design, as is requested by them.

4.1 Simple ship simulation (KCS case)

The first case study is to look at the total resistance for the Kriso container ship or KCS for short. The model included only the hull and no appendices. This is a ship design that many has used in academic studies. And the results from model towing tanks are published for use in academic work.

Many parameters need to be specified to do a complete simulation, but only a few needs to be specified by the user. The program specifies the rest of the default values. One important part that is chosen by default is the turbulence model. In ShipFlow, if nothing is specified it will use the EASM or Explicit Algebraic Stress Model. It is possible to change the turbulence model used, to either k-ω SST or k-ω BSL, if that suits the case better. Y^+ is another important parameter that can have a significant impact on the simulation. If nothing is stated for this keyword, the target value is set to 0.7. The program will then calculate the most correct value for different points along the hull based on the target value. An average is then represented at the end of the simulation together with the results. Generally in other CFD programs, the boundary conditions would be needed to be stated. This is not necessary for ShipFlow since the conditions are already prepared. It is therefore essential to know which way the ship is imported. So that the bow of the ship is facing the velocity outlet. A smaller parameter is water temperature. By changing this, the water density will also change. It is therefore important to have the same temperature in the simulation as in the model test

The ship hull CAD file could usually be downloaded from the internet. However, in this instance, it was already located in the files of ShipFlow. Because it was part of a tutorial. As a result of this, the offset file was already created. This made it easy just to try to implement a method for finding the total resistance. The main characteristics of KCS used in this case are shown in Table 4-1.

Table 4-1 Main dimensions of KCS (Zou & Larsson, 2014)

Scale Ratio = 31,6	Ship	Model
L_{PP} (m)	230	7,2786
B (m)	32,2	1,0190
T (m)	10,8	0,3418
Volume (m³)	52030	1,6490
C_b	0,6505	
C_m	0,9849	
LCB(%), fwd+	-1,48	

The method used to find the total resistance was with a VOF method. This was implemented to the program by choosing the Xpan and Xchap program and then implement the VOF function further down in the hull type section. The grid was selected to be fine and with a global mesh. This gave the cell distribution as shown in Table 4-2. The places that are described in Table 4-2 are illustrated in Figure 3-5 except for Etamax, which sets the number of planes in the circumferential direction. Also, Zetamax, which controls the number of planes in the radial direction. As well as Ytarget, which sets the target for y^+. The total amount of cells, in this case, differed from 3 million cells when the coarse mesh was used and up to 5 million cells when the fine mesh was used and the etamax and zetamax was tweaked to give a finer mesh.

Table 4-2 Mesh distribution and refinement zone

XSTART	-0,8		NU	45
XEND	1,8		NF	110
XFPU	-0,05		NM	130
XFPD	0,225		NA	45
XAPU	0,88		NW	50
XAPD	0,99		YTARGET	0,7
ETAMAX	70			
ZETAMAX	100			

An experimental test validated the simulation. This case was included to see if the program used could handle a model that is well tested and known. If the results from the simulation and experimental results are not within a certain similar degree, the method could not be used further. Which would mean that the method would need to be changed and refined, to more correctly simulate the model and get a more accurate result.

4.2 Vard ship simulation without appendices

The second case study is based on one of Vards own designs. And compares the resistance calculated from the computer simulation with the resistance measured from the towing tank test. The method used for this is different than what was used in the first case study. This is because Vard wanted to see how well one of the solvers in the program did compare to their measured model results. In the discussion, this will be elaborated further.

The main characteristics and shape of the ship are to be kept confidential at the request from Vard. However, what can be said is that it is a smaller ship than the KCS, and in this case, the model simulated are the same scale as the hull tested in the towing tank test.

To start the simulation, an earlier setup file was used together with the offset file provided by Vard. The setup file was also provided by Vard but needed to be changed. The full setup is shown in appendix 1 (setup). There it is possible to see the choices that were made. Such as only the program Xchap was used. As mentioned earlier, this is the one that uses the RANS-equation to simulate the flow around the ship hull.

Further, the speed needs to be specified. The parameter for speed in full scale needs to be given in knots, meter per second, or Froud number. In this case, the simulation was in model scale, so a scale needed to be stated as well. This is done by setting the correct reference length, scale, or Reynolds number. Speed in knots and scale factor was the parameter used. The reason for this was to be able to change the speed easy and minimizing the risk of inputting the wrong parameters.

For mesh size, the keyword "Fine" was used. This gave the same parameters as mentioned in Table 4-2. It was also assumed as sufficient from the contact person from Vard when he was asked about mesh size. With this keyword, the total number of cells amounted to 3,312,472. This correlates good with was mentioned in the assessment of the Gothenburg 2010 workshop. Where (Larsson & Zou, 2014) stated: "there is no error decrease above 3 M grid points." and "However, below 3 M cells the maximum error increase to about 8 %." This gives an estimate, but it should be noted that the workshop used the KCS ship. The mesh needed for a smaller vessel can then be assumed to be smaller.

To validate the results, different speeds where simulated. So that it is possible to compare the results with the model test results. The speed chosen was based on what was written in the towing test report so that the speed would overlap with the speed used in the towing test. The range of the speed was from a Froud number of 0,1392 and up to 0,2151. Every speed simulated needed its own setup, but the only difference in the setup was the change of speed.

The simulation ended when the program had achieved a good enough value in the standard deviation. If it had not achieved the value which was sat by default, it would have ran until it reached the maximum iterations. Which meant that some changes would be needed in the setup.

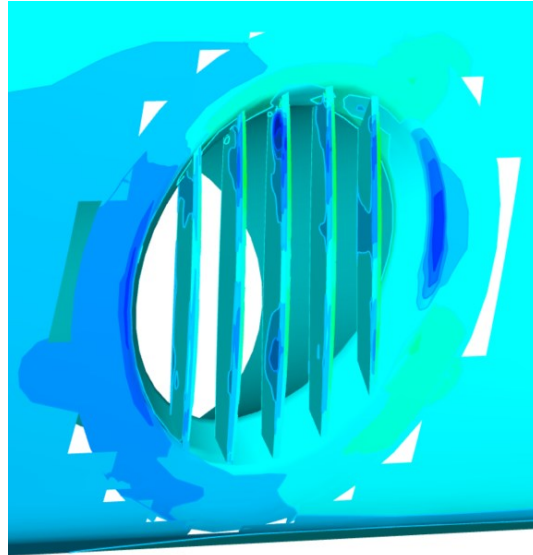## 4.3 Vard ship simulations with tunnel thruster

After simulating the hull with no appendices, the next step was to simulate with one appendix. In this case, that was the forward tunnel thruster. The same setup as used in 4.2 was used for this case as well, with just some modifications. The largest change is the implementation of the tunnel keyword. In this part, the characteristics of the thruster are specified. Such as the location, radius, length, dimensions of tunnel grids, tunnel rotation angle, Chamfer radial extent at 0, 90, and 180 degrees, Chamfer depth at 0, 90, and 180 degrees, number of bars, tunnel bars chord length, bar thickness, bar axial inward offset, bar angle from vertical, Dimensions of tunnel grid bar grids. Otherwise, the setup is the same. Ship Flow creates a grid in the existing model so that the model doesn't need to be changed in any other CAD program. After implementing the tunnel keyword and filled all the necessary parameters that were decided by Vard, the simulation was ran again. With the same speeds and speed increments used in the earlier case without a thruster.

After a completed simulation a representation of the tunnel can be viewed, and the thruster used in this case is shown in Figure 4-1 and Figure 4-2. The geometry of the thruster is shown, and it is possible to see how the grid is formed and if there are any inaccuracies. Something that could be of concern is the white areas around the thruster. However, after speaking with ShipFlow support, they assured that it was only a graphical flaw and would not impact the calculations.

Some of the problems that have risen during the implementation were that the bars leaked. When running the simulation, it would stop and give an error message that stated that the bars had leakage. This was first fixed by changing the offset on the bars. However, it was discovered that in an earlier version of the program, this fix did not work. But with the newest version, the problem disappeared. This is mentioned here because it is an important factor if the case should be recreated. Because it was one of the largest error sources when the simulation stopped.
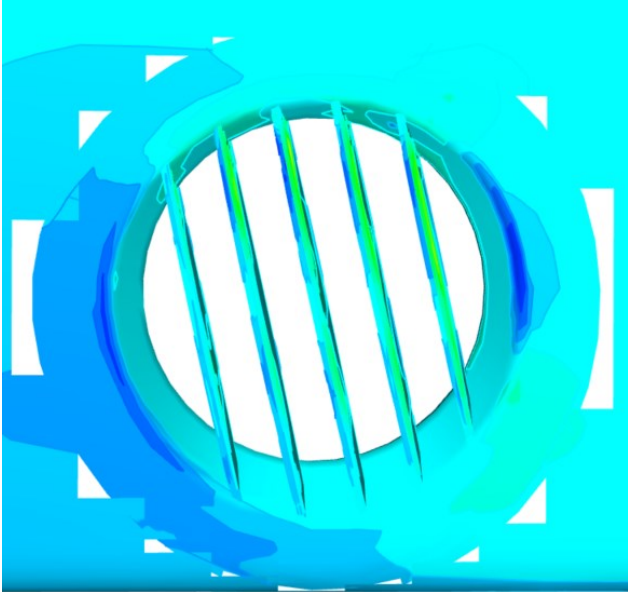
**Figure 4-1 Tunnel thruster implemented in ShipFlow, side view.**

Figure 4-2 Tunnel thruster in ShipFlow from an angled side view.

4.4 Vard ship simulations with different parameters on the tunnel thrusters

After establishing a method for both the ship with and without a thruster, the next step was to change the dimensions. By changing the dimensions, it might be possible to find a correlation for this ship with regards to size and speed for resistance.

The sizes investigated are from 70% and up to 110% from the original thruster size. With a size larger than 110% the thruster would need to be moved upwards to have room for the tunnel. Since moving the thruster is not within the scope of this thesis, this was not done. A smaller size than 70% was tried but did not work. Increments of 10% were used when testing the different sizes. The difference in size between the largest and smallest can be seen in Figure 4-3. The pictures are the same height, showing the top and bottom of the model.
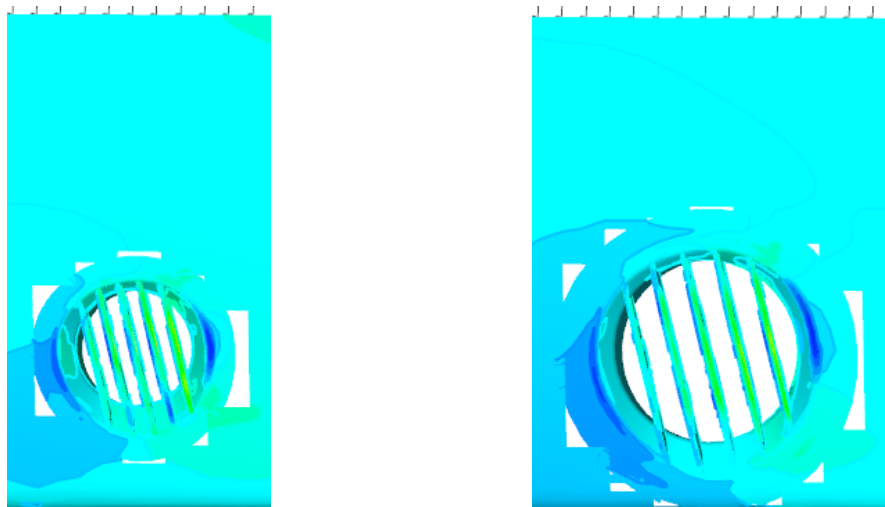
Figure 4-3 Illustration of the difference between the 70%- and the 110% thruster.

5 Results and discussion

This chapter will contain the results and discussion. Parts of the methodology and cases will be discussed, as well as the results. The results will mostly have dimensionless values so that the information given by Vard stays confidential. However, it still makes it possible to compare the results and discuss them.

ShipFlow was used as the CFD software to find the added resistance from the tunnel thruster. As a program, it was difficult in the beginning to learn how to operate all the different aspects. Such as how to convert a 3D model into the offset file that ShipFlow use, or getting the right visual representations needed to evaluate the meshes. However, after some time it became more intuitive. If standard cases and default values were used. However, when some problem arose, it was difficult to locate where the problem came from because of limited information. By the help of the support team, a lot of errors and problems got fixed. Changing parameters and implementing parameters was also difficult at times because the information on what to include and what type of unit the parameter used was hard to find and not in the user manual or tutorials.

In the first case, a KCS model was simulated. Since CFD simulation is a complex undertaking, a relatively simple and well-tested ship was therefore used to find a suitable method to use further. However, this was a rather large and time-consuming simulation. Early results are shown in Table 5-1, and are from a simulation using only the Xpan and Xchap programs, where the standard values were used except for Etamax and Zetamax. Which was increased to give a finer mesh since earlier simulations had a coarser mesh and were further from the test result values. As can be seen, the cell size is small, with almost 5 million cells. This should be enough cells considered what was studied at the Gothenburg 2010 workshop mentioned in chapter 4.2. However, the resistance values differed with above 18 % from the model test, which meant that the method was not good enough. The resistance values used to compare with was from a paper on measurement of flows around modern commercial ship models (Kim, Van, & Kim, 2001).

Table 5-1 Result from KCS, standard solver.

Speed [Fn]	Cell number	Ct	Difference [%]	Time [hh:mm]
0,26	4964526	0,004211	18,38628057	05:30
0,26	4370190	0,004222	18,69552994	03:54

To improve the resistance calculation, a VOF solver was added, while still using the same general mesh size. This improved the result so much that the difference between the model test and the simulation for that single case went down to only 1,6 %. However, after speaking with the contact person at Vard, this method could not be used for later cases since it did not include the appendage calculations needed later. Which also was what Vard was interested in testing. No more simulation was done on the KCS model since the wrong solver would be needed to find good results, and comparing results and to a mesh sensitivity study with the earlier setup would be time-consuming.

All the following cases which included the Vard ship models, only used the Xchap part of ShipFlow, since this part also included appendages in the calculations. The reason for only using Xchap was that it mainly calculated the viscous forces on the hull. So if the thruster were far enough below the surface, it would not influence the wave resistance of any considerable importance, and therefore only contribute to the viscous forces. This was validated by the contact person at Vard. Since he witnessed the towing tank test, and the wave pattern was approximately the same. Xpan was chosen not to be included since it solves the potential problems, and therefore would not contribute to the appendage resistance, but use more computational time.

The Vard model simulated, was scaled down to the same size as the towing tank model. This was to save computational power, by calculating in a lower Reynolds number. It also meant that the results did not need to be scaled from model to full scale to be compared.
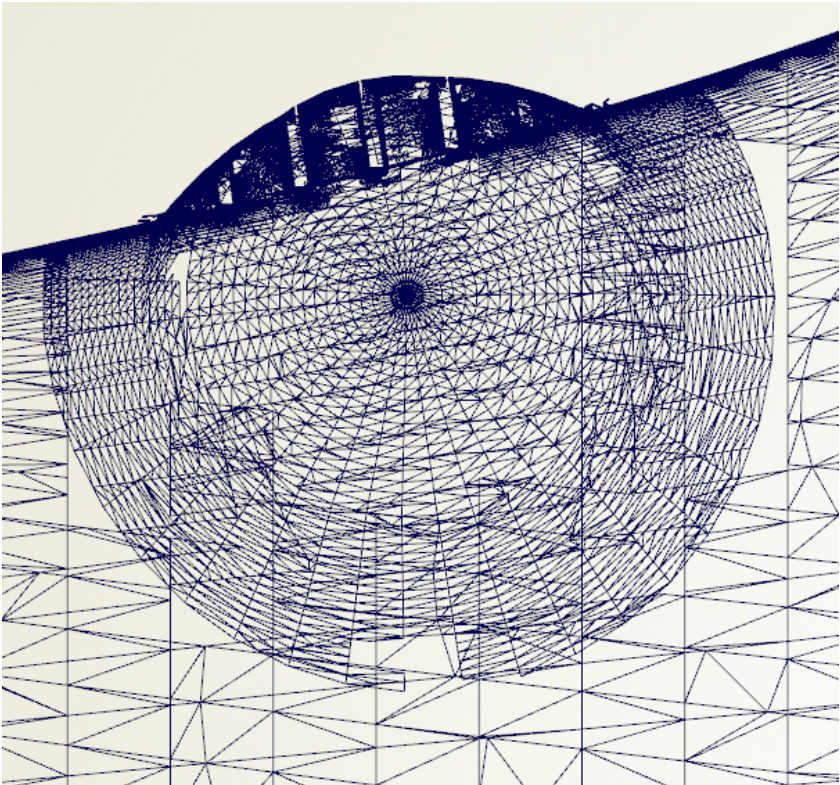
Figure 5-1 Illustration of the mesh around the tunnel in XZ-plane.

Mesh size was chosen as mentioned earlier, but because of long simulation time, the mesh was reduced to medium size. This was because it was noted that it had enough cells to be viable in regard to the Gothenburg workshop. With a smaller mesh size, the computational time was greatly decreased. This helped a lot in the end since it made it possible to get some more results. After a couple of different speeds with different tunnel, sizes was simulated, the few cases with a finer grid were simulated again but with the same quality of mesh as the other simulation. The difference in the number of cells, time used, and the dimensionless resistance can be seen in Table 5-2. Here it is possible to see that the difference is not that great, but when the resistance from the thruster is isolated and compared, the difference is easier to spot. As is done in Figure 5-2. A mesh convergence study should have been done to find out how large impact the cell size had. An investigation into refining the mesh could be beneficial. As shown in Figure 5-1, the mesh around the tunnel thruster is chaotic and not reliable. This might be a visual bug, but it is hard to know without looking further into the case.

Table 5-2 Results from a Froud number of 0,1772, where the upper part has medium mesh, and the lower portion has a fine mesh.

Radius [%]	Nr. cells	Iteration	Time [hh:mm:ss]	CT * E3
-	3011712	111	00:42:28	2,948
100	3046328	151	00:54:10	3,032
90	3042688	111	00:41:14	3,018
80	3030779	181	01:04:51	2,999
70	3016219	131	00:47:36	3,001
-	3312472	111	01:43:43	2,947
110	4241103	131	02:54:03	3,054
100	4238452	500	12:51:46	3,002
90	4234812	161	04:09:52	3,027
80	4219262	191	04:44:49	2,989
70	4208343	121	02:52:40	2,991

The simulation only calculates the viscous forces, for a total resistance that would not be good enough but when the difference between the resistance with and without thruster are investigated, this is assumed to be close enough. There will be a difference in the total resistance between the model test and CFD. However, the additional tunnel thruster resistance should be the same. But because of the difference in total resistance, a percentage difference would wrongfully represent the additional resistance a tunnel would give, so, the results are shown in dimensionless values, to take this into account. By showing them as dimensionless, the confidentiality is maintained, and the results can be compared to other studies at a later date.

The results from the simulation with and without the tunnel thruster are shown in Figure 5-2. It is showing the dimensionless resistance difference between the model tested with and without the thruster. This was done because the total resistance differed substantially as mentioned in the part above. It is possible to see a downward trend for the blue line which represents the experimental results, and this is weird because the other blue line in Figure 5-3 which represents a different model showed an upward trend. If both graphs are converted into Newton, the first will almost be a straight horizontal line, while the second graph will have an exponential growing graph.

The orange line from the first figure shows the results from the simulation with the original tunnel. It showed that the dimensionless resistance does not have an increasing or decreasing trend, but it varies somewhat between the different data point. The difference in the two cases are discussed further below in the part under the Table 5-3, but since the tolerance of the experimental results are ±0.5 %, and the tunnel thruster contribution is only around 1-3 % the results listed below are assumed good enough. A better grid might have given more accurate results from some of the speeds. However, because of lack of computer power, it was to time demanding to redo many of the simulations and run enough simulations to get enough to conclude later. The second graph was included to show that there might be some error in the experimental tests done.

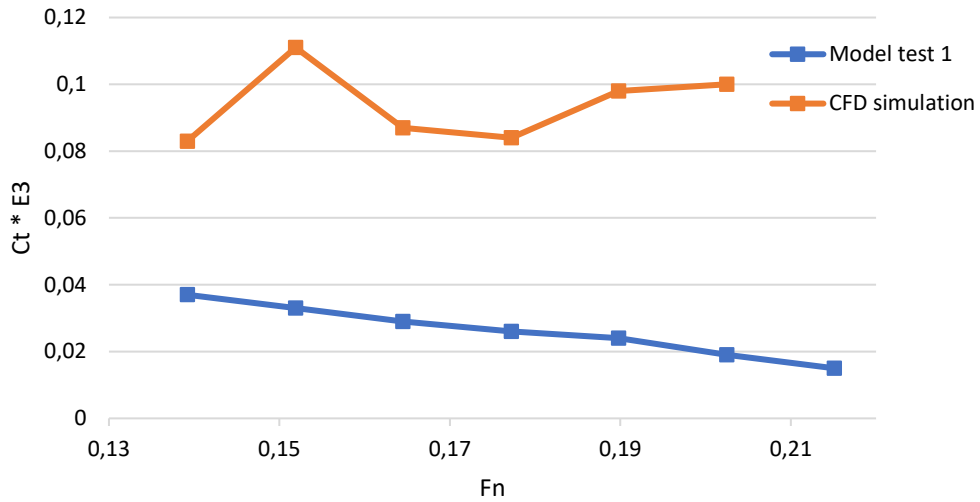## Comparision of model test and CFD w/o thruster

Figure 5-2 Appendage resistance contribution on the total resistance for model 1.

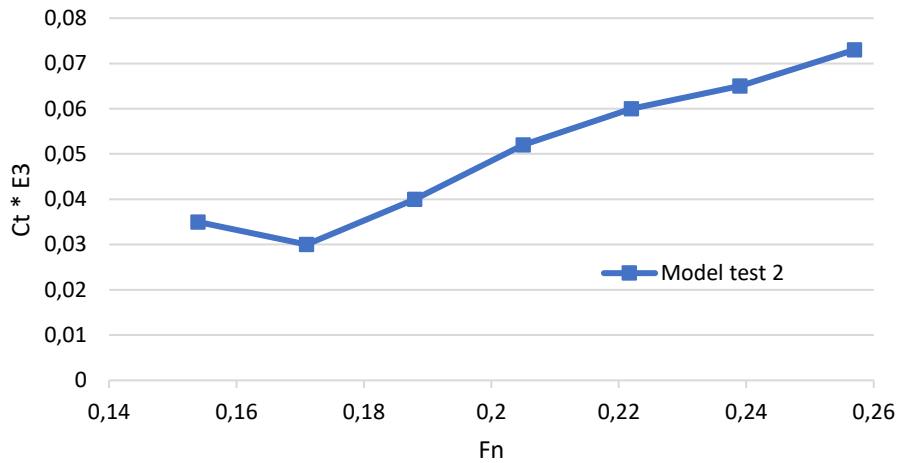## Comparision of model test and CFD w/o thruster

Figure 5-3 Appendage resistance contribution on the total resistance for model 2.

Table 5-3 Showing the difference between the experimental and simulation results relative to the total resistance of a ship without a thruster.

Speed [Fn]	Percentage difference
0,1392	1,39 %
0,1519	2,36 %
0,1645	1,76 %
0,1772	1,76 %
0,1898	2,24 %
0,2025	1,95 %

The difference between the experimental and the results from the simulation shown in Figure 5-2 are shown in Table 5-3. This was calculated by finding the difference between the difference of the experimental with and without, and the difference of the CFD with and without the thruster. Then divided it by the experimental total resistance for the simulation with a tunnel. So that it is possible to see the difference between the simulation and the experimental relative to the total resistance.

Additional resistance from different thruster sizes
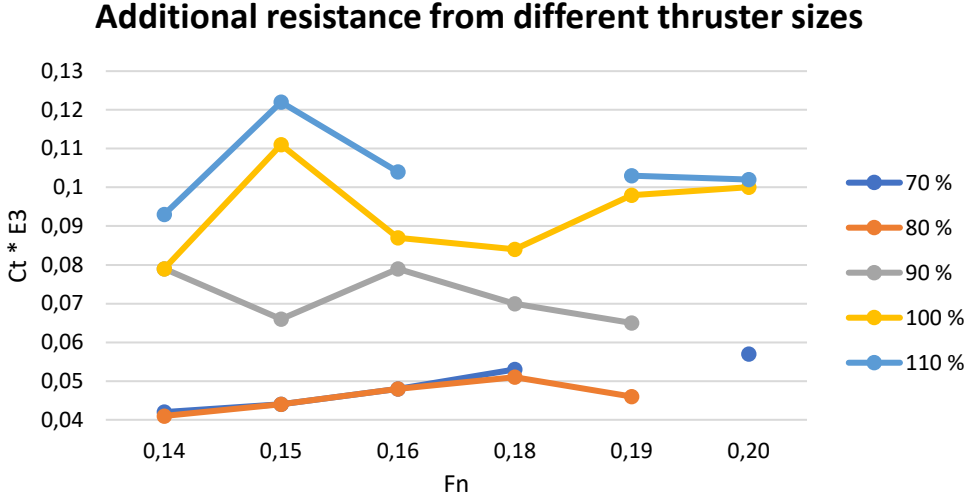
Figure 5-4 Additional resistance of different tunnel sizes with regards to speed.

Figure 5-4 above shows the different added resistances from different size of the same tunnel thruster. The lines were used to fine a correlation between the size and added resistance of a vessel, but since there are so few data points, and only tested for one ship, the correlation could be bad for other ships. However, as is shown in Figure 5-5, the estimate based on the results shown earlier is better at predicting the added resistance for the second model from Vard compared to the Holtrop method. By changing the Holtrop equation that calculated the tunnel resistance, to an equation that found the coefficient based on resistance, speed, and radius. It was possible to find a coefficient like the one that Holtrop has, and the comparison is shown below. The coefficient found from all the CFD results was 0,00174592. And by using Holtrop's formula for Tunnel thruster resistance, but with the new coefficient, the estimate became what is shown with the grey line.

Added thruster resistance estimate
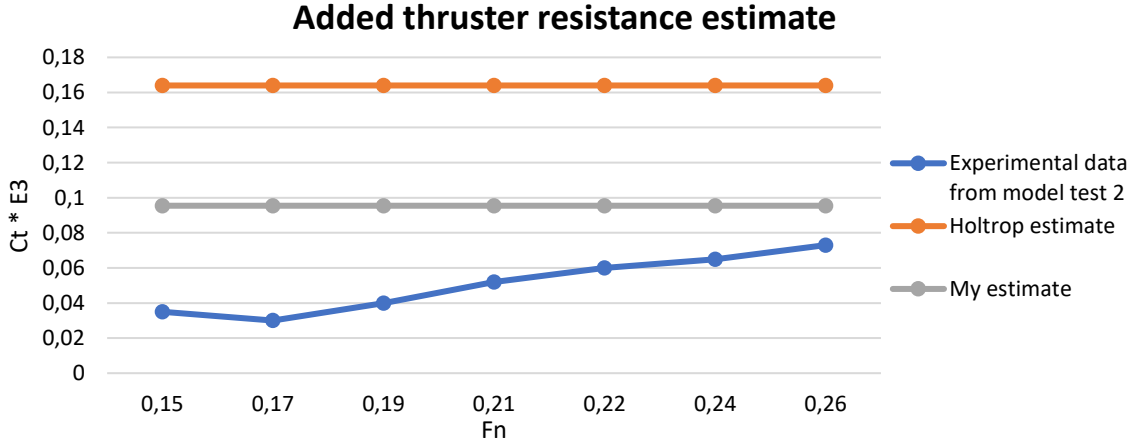
Figure 5-5 Comparison between methods to estimate the added resistance from a tunnel thruster.

6 Concluding remarks

After looking at the process of setting up a CFD simulation and then comparing the results with a towing tank test, it is possible to find the estimated resistance from both experimental and computational simulation. However, as seen earlier, both methods have their flaws and inaccuracies. One cannot trust blindly on each individually. Therefore is it important to have other data from similar designs to compare with, so one can validate the results to some degree.

By using the formula from Holtrop and calculating a new coefficient, it was possible to establish a simple and practical relation between appendage size and the added resistance on a ship. However, to know if it is reliable, more testing would need to be done on other test cases with known towing test results. The method used in the CFD simulations also needs further investigation to find a more accurate method to find the resistance. However, with a more accurate method, the coefficient used will most likely get more correct in estimating the resistance. The method used now still have potential for improvements, but it was nevertheless more accurate than the old method from Holtrop.

6.1   Future works

The topics in this thesis have still areas to explore. By using CFD to find a new coefficient, shows that it is possible to renew some of the old formulas, without doing too many model trials. It can be possible to improve some of the equations by changing other parameters in the design and find new relations. One of the parameters that would be interested too look into are the angle of the tunnel chamfer at the end of the tunnel. It would also be interested to see how this method could be used for other appendages, such as stabilizing fin cut-outs.

To improve the method used, a mesh sensitivity study should be conducted, together with an investigation for the refinement zone around the thruster. All of those topics mentioned could be future work either individually or combined.

References

Bertram, V. (2012). Chapter 1 - Introduction. In V. Bertram (Ed.), *Practical Ship Hydrodynamics (Second Edition)* (pp. 1-39). Oxford: Butterworth-Heinemann.

Bhaskaran, R., & Collins, L. (2002). Introduction to CFD basics. *Cornell University-Sibley School of Mechanical and Aerospace Engineering*, 32.

Carlton, J. (2012). *Marine Propellers and Propulsion* (3 ed.): Elsevier Science.

Carlton, J. S. (2007). 12 - Ship resistance and propulsion. In J. S. Carlton (Ed.), *Marine Propellers and Propulsion (Second Edition)* (pp. 286-318). Oxford: Butterworth-Heinemann.

El Moctar, B. (2008). *State-of-the-Art CFD Simulation for Ship Design* (Vol. 124). Berlin, Heidelberg: Springer Berlin Heidelberg.

Flowtech. (2019). Shipflow 6.4 users manual. In.

George R. Stuntz, R. J. T. (1964). Some Aspects of Bow-Thruster Design. *THE SOCIETY OF NAVAL ARCHITECTS AND MARINE ENGINEERS, no. 6*.

Hochhaus, D. K.-H. (Producer). (2012, 05.02.19). Innovation 3-Querstrahler im-Bug. Retrieved from https://upload.wikimedia.org/wikipedia/commons/1/12/2012_09_03_Innovation_3-Querstrahler_im-Bug_2kk_DSCI0786.JPG

House, D. J. (2007). *Ship handling : theory and practice*(1st ed. ed.).

ITTC. (2002). Testing and Extrapolation Methods Resistance Test. In: International Towing Tank Conference. Recommended Procedures 7.5-02-02-01.

Kim, W. J., Van, S. H., & Kim, D. H. (2001). Measurement of flows around modern commercial ship models. *Experimental Methods and their Applications to Fluid Flow, 31*(5), 567-578. doi:10.1007/s003480100332

Larsson, L., & Zou, L. (2014). Evaluation of Resistance, Sinkage and Trim, Self Propulsion and Wave Pattern Predictions. In L. Larsson, F. Stern, & M. Visonneau (Eds.), *Numerical Ship Hydrodynamics: An assessment of the Gothenburg 2010 Workshop* (pp. 17-64). Dordrecht: Springer Netherlands.

Menter, F. R. (1994). Two-equation eddy-viscosity turbulence models for engineering applications. *AIAA Journal, 32*(8), 1598-1605. Retrieved from https://arc.aiaa.org/doi/abs/10.2514/3.12149. doi:10.2514/3.12149

Molland, A. F., Turnock, S. R., & Hudson, D. A. (2011). *Numerical Estimation of Ship Resistance*. Cambridge: Cambridge University Press.

Molland, A. F., Turnock, S. R., & Hudson, D. A. (2011). Ship Resistance and Propulsion. In (pp. 12-68): United Kingdom: Cambridge University Press.

Petersson, N. A., & Chand, K. K. (2001). *Detecting translation errors in CAD surfaces and preparing geometries for mesh generation*. Retrieved from

Wärtsilä (Producer). (2019, 05.02.19). Wärtsilä Retractable Thrusters. Retrieved from https://www.wartsila.com/marine/build/propulsors-and-gears/thrusters/wartsila-retractable-thrusters

Zou, L., & Larsson, L. (2014). Additional Data for Resistance, Sinkage and Trim. In L. Larsson, F. Stern, & M. Visonneau (Eds.), *Numerical Ship Hydrodynamics: An assessment of the Gothenburg 2010 Workshop* (pp. 255-264). Dordrecht: Springer Netherlands.

Appendices

1. Setup file for one of the simulation for a Vard ship without tunnelthruster.

Setup

Setup file for one of the simulation for a Vard ship without tunnelthruster.

```
xflow
title( title = "SHIPFLOW" )
program( xcha )
vship( vknot = 14, scale = xx.xx )
hull( mono, h1gr = "main", fbgr = "bulb", wtran )
offset( file = "as_as_off_xxxx_R12", lpp = xxx, zori = x.x )
fluid( fresh, temp = 20.5 )
end

xgrid
size( fine, global )
xdistr( nf = 150 )
singul( keel, xyzfwd = [2.721755,0,0.357788] )
end

xchap
control( start, maxit = 500 )
end

xpost
control( off )
end
```